

ARL-TR-85-3

Copy No. 8

(2)

THE MOVING THERMOACOUSTIC ARRAY:  
A THEORETICAL FEASIBILITY STUDY

Nicholas P. Chotiros

AD-A154 510

APPLIED RESEARCH LABORATORIES  
THE UNIVERSITY OF TEXAS AT AUSTIN  
POST OFFICE BOX 8029, AUSTIN, TEXAS 78713-8029

17 January 1985

Technical Report

APPROVED FOR PUBLIC RELEASE;  
DISTRIBUTION UNLIMITED.

*Proceedings*

OFFICE OF NAVAL RESEARCH  
DEPARTMENT OF THE NAVY  
ARLINGTON, VA 22204

DTIC  
SELECTED  
JUN 4 1985  
S E D

DTIC FILE COPY



20000814040

85 5 02 001

# UNCLASSIFIED

SECURITY CLASSIFICATION OF THIS PAGE (When Data Entered)

REPORT DOCUMENTATION PAGE		READ INSTRUCTIONS BEFORE COMPLETING FORM
1. REPORT NUMBER	2. GOVT ACCESSION NO. <b>A154570</b>	3. RECIPIENT'S CATALOG NUMBER
4. TITLE (and Subtitle) THE MOVING THERMOACOUSTIC ARRAY: A THEORETICAL FEASIBILITY STUDY	5. TYPE OF REPORT & PERIOD COVERED technical report	
7. AUTHOR(s) Nicholas P. Chotiros	6. PERFORMING ORG. REPORT NUMBER ARL-TR-85-3	
9. PERFORMING ORGANIZATION NAME AND ADDRESS Applied Research Laboratories The University of Texas at Austin Austin, Texas 78713-8029	8. CONTRACT OR GRANT NUMBER(s) N00014-82-K-0425	
11. CONTROLLING OFFICE NAME AND ADDRESS Office of Naval Research Department of the Navy Arlington, Virginia 22217	10. PROGRAM ELEMENT, PROJECT, TASK AREA & WORK UNIT NUMBERS	
14. MONITORING AGENCY NAME & ADDRESS (if different from Controlling Office)	12. REPORT DATE 17 January 1985	
	13. NUMBER OF PAGES 62	
16. DISTRIBUTION STATEMENT (of this Report)  Approved for public release; distribution unlimited.	15. SECURITY CLASS. (of this report) UNCLASSIFIED	
	15a. DECLASSIFICATION/DOWNGRADING SCHEDULE	
17. DISTRIBUTION STATEMENT (of the abstract entered in Block 20, if different from Report)		
18. SUPPLEMENTARY NOTES		
19. KEY WORDS (Continue on reverse side if necessary and identify by block number)		
20. ABSTRACT (Continue on reverse side if necessary and identify by block number) A theoretical study of the feasibility of the moving thermoacoustic source as a sound projector in underwater acoustic applications is presented. Since the Doppler shift is direction dependent, it was found that the moving optoacoustic sources are potentially useful for direction finding by virtue of the extremely high Doppler shifts achievable. While the thermoacoustic array has certain advantages over conventional acoustic projectors, notably the noncontact property and the Doppler direction finding capability, its optoacoustic energy conversion efficiency is no better than that of the stationary thermoacoustic array. This		

## UNCLASSIFIED

20. (cont'd)

conclusion was arrived at through mathematical analysis from basic principles, and supported by computer generated numerical examples. The conversion efficiency was found to be strongly dependent on the acoustic signal carrier frequency and on the optical signal waveform. It was found that the thermoacoustic conversion was most efficient when the optical energy was delivered as an impulse train. The efficiency is fundamentally limited by the physical properties of the medium, particularly the coefficient of thermal expansion and the specific heat. A different optoacoustic conversion process, which employs nonlinear physical reactions to generate sound, is being pursued.



Accession For	
NTIS GRA&I	<input checked="" type="checkbox"/>
DTIC TAB	<input type="checkbox"/>
Unannounced	<input type="checkbox"/>
Justification	
By _____	
Distribution/	
Availability Codes	
Dist	Avail and/or Special
A/1	

## TABLE OF CONTENTS

	Page
LIST OF FIGURES	v
SYMBOL TABLE	vii
SUMMARY	1
I. INTRODUCTION	3
II. OBJECTIVES	7
III. THEORY	9
A. Basic Theory	9
B. The Moving Thermoacoustic Array	11
C. The Stationary Thermoacoustic Array	12
IV. THE EFFECT OF MOVEMENT ON THE OPTICAL ENERGY REQUIREMENT	15
A. The $M \neq 1$ Case	16
B. The $M = 1$ Case	20
V. ANALYSIS OF VIABILITY AS AN ACOUSTIC PROJECTOR	23
A. Upper Bound of the Energy Density	23
B. Waveform and the Energy Conversion Efficiency $M \neq 1$	26
C. Maximization of the Signal-to-Noise Ratio	28
D. Conversion Efficiency Upper Bound	29
VI. NUMERICAL EXAMPLES OF MOVING THERMOACOUSTIC SOURCE	33
VII. DIRECTION FINDING CAPABILITY	39
VIII. FINDINGS	41
IX. DISCUSSION	43

	<u>Page</u>
<b>H. CRITICAL ISSUES</b>	<b>45</b>
<b>A. Efficiency Enhancement</b>	<b>45</b>
<b>B. Planned Work</b>	<b>45</b>
<b>APPENDIX A. BASIC THERMOACOUSTIC GENERATION THEORY</b>	<b>47</b>
<b>APPENDIX B. MAXIMUM OPTICAL POWER FOURIER TRANSFORM</b>	<b>53</b>
<b>REFERENCES</b>	<b>57</b>

## LIST OF FIGURES

<u>Figure No.</u>	<u>Title</u>	<u>Page</u>
1	Geometry of the Moving Thermoacoustic Source	10
2	Frequencies at which Upper Bounds of Energy Density and Signal-to-Noise Ratio are Maximized	25
3	Three Waveforms and their Power Density Spectra	27
4	Energy Conversion Efficiency Upper Bound in Seawater at a Temperature of 10°C	32
5	The Computed Slant Range Penetration of a Moving Thermoacoustic Array (MTA), Traveling at $M=0.9$ in the Indicated Direction	34
6	The Computed Slant Range Penetration of a Stationary Thermoacoustic Array Generating an Acoustic Signal at 20 kHz	36
7	The Geometry of a General Stationary Thermoacoustic Array	52

## SYMBOL TABLE

**Latin :**

<b>a</b>	1/e radius of the Gaussian shaded light beam (m)
<b>R</b>	optical transmissivity of the liquid surface
<b>B<sub>a</sub></b>	acoustic signal bandwidth (Hz)
<b>c</b>	speed of sound in water (m/sec)
<b>C<sub>a</sub></b>	thermoacoustic conversion factor
<b>c<sub>p</sub></b>	specific heat of water (J kg <sup>-1</sup> °C <sup>-1</sup> )
<b>D<sub>a</sub></b>	loss term for optical reflection loss and acoustic diffraction loss
<b>D<sub>ao</sub></b>	mean loss term for optical reflection loss and acoustic diffraction loss over the significant part of the path
<b>DI<sub>r</sub></b>	directivity index of the receiver (dB)
<b>DI<sub>t</sub></b>	directivity index of the transmitter (dB)
<b>E<sub>a</sub></b>	acoustic energy density flux (J m <sup>-2</sup> )
<b>F<sub>N</sub></b>	equivalent plane wave isotropic noise spectral density
<b>I</b>	optical intensity flux vector (W m <sup>-2</sup> )
<b>k</b>	wave number of acoustic signal (m <sup>-1</sup> )
<b>k<sub>0</sub></b>	mean wave number of acoustic signal (m <sup>-1</sup> )
<b>M</b>	Mach number
<b>MTR</b>	moving thermoacoustic array
<b>P<sub>a</sub>(ω)</b>	Fourier transform of acoustic pressure (Pa sec rad <sup>-1</sup> ) thermoacoustic source (Pa sec rad <sup>-1</sup> )

$r$	source-receiver distance measured from the intersection of the laser beam axis and the surface to the receiver (m)
$r_0$	mean value of $r$ over the significant part of the path
S/N	signal-to-noise ratio (dB)
TR	thermoacoustic array
$T_c$	acoustic pulse length (sec)
$T_0$	optical pulse duration (sec)
$t$	time (sec)
$W(\omega)$	Fourier transform of optical power of a moving thermoacoustic source ( $W \text{ sec rad}^{-1}$ )
$W_0(\omega)$	Fourier transform of optical power of a stationary source ( $W \text{ sec rad}^{-1}$ )
$w(t)$	optical power input of a moving thermoacoustic source (W)
$w_0(t)$	optical power input of a stationary thermoacoustic source (W)
$R$	coefficient of thermal expansion of water ( $^{\circ}\text{C}^{-1}$ )
$x(t)$	$x$ coordinate of the MTR on the surface (m)
$y(t)$	$y$ coordinate of the MTR on the surface (m)
$Z_0$	plane wave acoustic impedance ( $\text{kg sec m}^{-2}$ )

**Greek :**

- $\alpha$  absorption coefficient of sound in water ( $\text{Np m}^{-1}$ )
- $\mu$  absorption coefficient of light in water ( $\text{Np m}^{-1}$ )
- $\phi$  azimuth angle relative to forward motion (rad)
  
- $\theta$  depression angle measured from the intersection of the laser beam axis and the surface to the receiver (rad)
- $\theta_0$  mean value of  $\theta$  over the significant part of the path
- $\rho$  density of water ( $\text{kg m}^{-3}$ )
- $\Omega$  solid angle (steradian)
- $\omega$  frequency ( $\text{rad sec}^{-1}$ )

## SUMMARY

A theoretical study of the feasibility of the moving thermoacoustic source as a sound projector in underwater acoustic applications is presented.

The thermoacoustic process employs direct heating of the acoustic medium to produce a controlled local thermal expansion which, in turn, generates sound waves. The thermal energy is delivered by a laser beam to the water surface without any physical contact. The analysis in this report is limited to the thermoacoustic conversion process, within the broader class of optoacoustic processes. The thermoacoustic source may be moved by deflecting the laser beam. A rotating mirror is commonly used to deflect the beam. The deflection causes the position of the thermal sound source to change as a function of time. This allows the signal to be Doppler shifted to a degree far greater than that achievable with conventional sound projectors that have to be in physical contact with the acoustic medium.

A summary of the findings presented in this report is as follows. Since the Doppler shift is direction dependent, it was found that the moving optoacoustic sources are potentially useful for direction finding by virtue of the extremely high Doppler shifts achievable. While the thermoacoustic array has certain advantages over conventional acoustic projectors, notably the noncontact property and the Doppler direction finding capability, its optoacoustic energy conversion efficiency is no better than that of the stationary thermoacoustic array. This conclusion was arrived at through mathematical analysis from basic principles, and supported by computer

generated numerical examples. The conversion efficiency was found to be strongly dependent on the acoustic signal carrier frequency and on the optical signal waveform. Studies of the effect of optical input signal characteristics on the conversion efficiency, the efficiency upper bound, and the projected range penetration under oceanic conditions were made. It was found that the thermoacoustic conversion was most efficient when the optical energy was delivered as an impulse train. It was concluded that the thermoacoustic array, within the broader category of optoacoustic processes, is expected to be useful as a laboratory tool where relatively high ultrasonic frequencies are used, but not for sonar applications because of the low thermoacoustic conversion efficiency in the useful range of sonar frequencies. The efficiency is fundamentally limited by the physical properties of the medium, particularly the coefficient of thermal expansion and the specific heat. A different optoacoustic conversion process, which employs nonlinear physical reactions to generate sound, is being pursued. It promises to be more efficient by several orders of magnitude.

## I. INTRODUCTION

A "thermoacoustic" source is realized when heat is directed into a small region of an acoustic medium. The thermal expansion or contraction of the medium causes a volumetric change which propagates as an acoustic wave outwards from the heated region. Since the thermal source is often generated optically, it is sometimes referred to as a "thermo-optical" source. The optically generated thermoacoustic source also belongs to the broader class of "optoacoustic" sources. These terms may be used interchangeably, except in those cases where their differences are important.

In 1976 the process was investigated theoretically and experimentally by Muir, Culbertson, and Clyne<sup>1</sup> for the case of a stationary source. The acoustic energy produced by the thermoacoustic array, (TA), with any reasonable quantity of optical energy through the thermoacoustic conversion process, was found to be small. It was several orders of magnitude smaller than that produced by conventional acoustic sources under equivalent operating conditions.

It is stated by Lyamshev and Naugol'nykh<sup>2</sup> in a comprehensive review paper that

"Under the conditions of thermo-optical generation of sound (i.e., the thermal mechanism) the conversion efficiency attains at best  $10^{-5} - 10^{-6}$ ."

Therefore, for underwater detection and communication purposes, the thermoacoustic conversion efficiency must be significantly increased before the TA can be considered as a viable acoustic source. There have been several recent Soviet papers on the subject with diverse claims, particularly with regard to the moving thermoacoustic source.

It was suggested by some that the moving thermoacoustic source, (MTR), can give significantly higher conversion efficiencies. The simplest case is that of an MTR traveling in a straight line. Here Bozhkov et al.<sup>3</sup> claim that moving thermo-optical sources are

"highly directional sound sources with a tunable frequency and considerably higher efficiency than that of stationary sources."

in an earlier publication, Bozhkov et al.<sup>4</sup> also claimed that

"the given method of sound generation affords a realistic possibility for the creation of powerful short pulses with a high frequency carrier."

The case of an MTR executing various types of motion, including oscillatory motion, has been studied by Lyamshov and Sedov,<sup>5</sup> but they claim, only that the efficiency of moving sources is

"practically the same as for a stationary source."

It is against this background of diverse and conflicting claims regarding the performance of the MTR that the investigation takes place.

An overview of the report is briefly as follows.

The thermoacoustic conversion process is analyzed from basic principles in section 3. Both the stationary and moving cases are examined. The special case of a Mach number of unity is also treated. The conversion efficiencies are compared in section 4. The influence of the optical signal waveform and the acoustic signal frequency on the conversion efficiency is examined and then the energy conversion efficiency upperbounds are established in section 5. The

performance of the thermoacoustically generated signal, particularly range penetration under typical oceanic conditions, is analyzed, supported by numerical examples, in section 6. The direction finding capability is discussed in section 7. The findings are discussed and compared with the claims quoted above in sections 8 and 9. Finally, the remaining critical issues and the methods to resolve them are discussed in section 10.

## II. OBJECTIVES

1. The thermoacoustic process and its conversion efficiency will be investigated from first principles.
2. The upper limit of the conversion efficiency and the factors which affect it will be determined.
3. The claims that have been made for the thermoacoustic process in the open literature will be examined.
4. The viability of the thermoacoustic source as a projector of acoustic signals in underwater acoustic applications will be assessed.

### III. THEORY

#### A. Basic Theory

In this study, the medium is water and the means of introducing heat is a laser. The thermal input may be controlled by modulating the laser power. The absorption coefficient of light in water is assumed to be uniform. Therefore, the thermoacoustic source is exponentially tapered as a function of penetration distance into the water. The geometry is shown in Fig. 1.

A suitable starting point is the expression for the Fourier transform of the farfield acoustic pressure generated by a stationary TA such as the one derived by Lyamshev.<sup>2</sup> Lyamshev's expression was for a lossless medium but in the following expression, which is derived in Appendix A, the absorption coefficient is included.

$$P_{\theta\theta}(\omega) = k C_{\theta} D_{\theta} W_{\theta}(\omega) \exp(ikr_{\theta} - \alpha r_{\theta}) / r_{\theta}, \quad (1)$$

where

$$C_{\theta} = \beta H c / (4\pi C_p) \quad (2)$$

and

$$k = \omega / c. \quad (3)$$

The parameters  $C_{\theta}$  and  $D_{\theta}$  have the following significances.  $C_{\theta}$  represents the thermoacoustic conversion factor afforded by the physical properties of the medium.  $D_{\theta}$  represents the acoustic losses due to diffraction caused by the

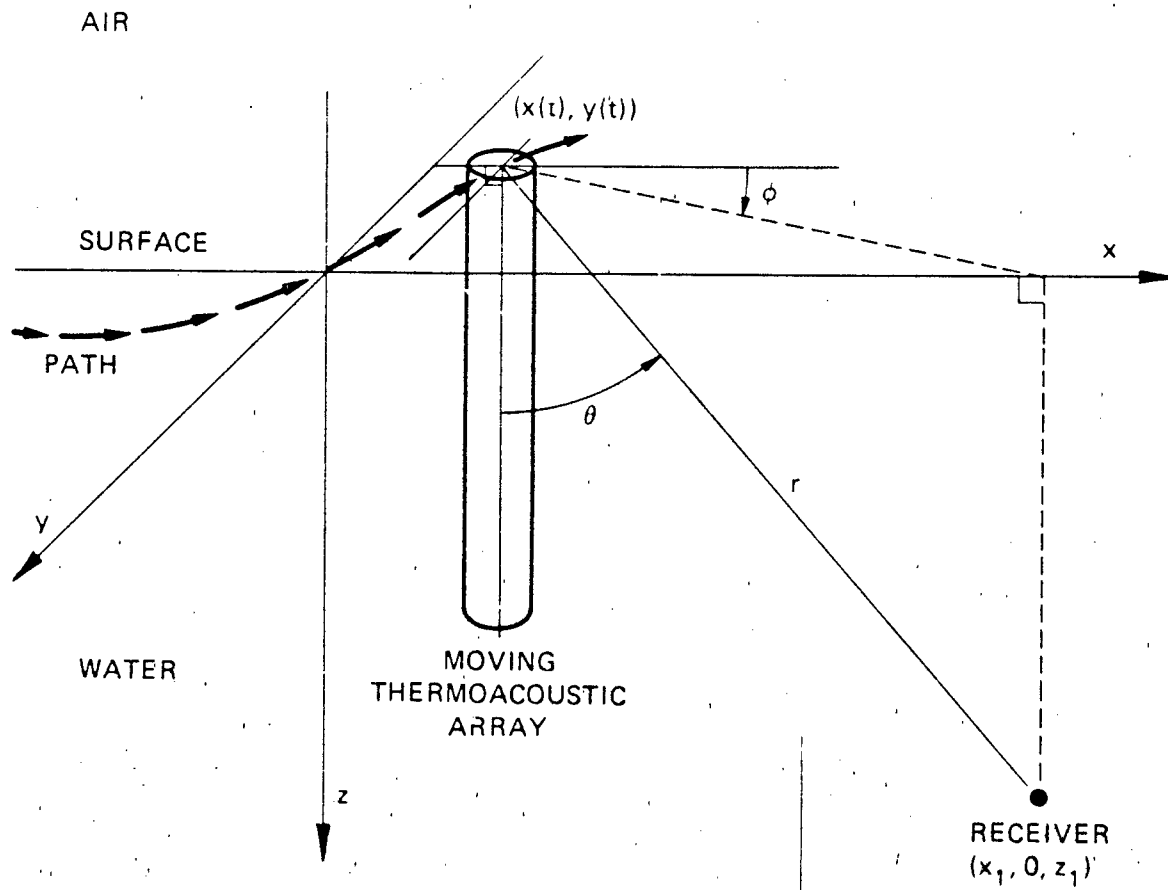


FIGURE 1  
 GEOMETRY OF THE MOVING THERMOACOUSTIC SOURCE

finite array length and width, and the optical loss due to reflection at the surface. In addition to the general case, the special case where the optical beam is vertical and the intensity profile in the horizontal plane is a Gaussian function is worth considering because it is capable of yielding a closed form solution; in this case,  $D_a$  is given by<sup>2</sup>

$$D_a = \mu k \cos \theta \exp(-k^2 a^2 \sin^2 \theta / 4) / (\mu^2 + k^2 \cos^2(\theta)), \quad (4)$$

where  $a$  is the  $1/e$  radius of the Gaussian function.

The response to an optical impulse is easily obtained by equating  $W_0(\omega)$  to the Fourier transform of an impulse.

### B. The Moving Thermoacoustic Array

Let us now consider the case of an MTR. The MTR will be modeled as a continuum of stationary optical impulses distributed along its path in space and time. Let the water surface be the  $x$ - $y$  plane in a Cartesian coordinate system, as shown in Fig. 1. The top end of the MTR must always be at the water surface. Let the changes in its  $x$  and  $y$  coordinates as a function of time be described by path functions  $x(t)$  and  $y(t)$ , where the time  $t$  is the independent variable, and let the path be centered at the origin. Therefore, the response of an MTR of arbitrary path function and an optical power input function  $w(t)$  may be formulated as a convolution of the impulse response and the source distribution function in space and time. Since time is the independent variable,

the result may be expressed as the time integral

$$P_a(\omega) = k C_a D_a \int_{-\infty}^{\infty} \omega(t) \exp(ik[r - ct] - \alpha r) / r \, dt, \quad (5)$$

where  $r$ , as shown in Fig. 1, is the distance from the surface-end position of the MTA at  $(x(t), y(t), 0)$  to the receiver position at  $(x_1, 0, z_1)$ . It is implicit that  $r$  varies as a function of  $t$ . The acoustic pressure  $p_a$  may be obtained by taking the inverse transform

$$p_a(t) = \int_{-\infty}^{\infty} P_a(\omega) \exp(-j\omega t) \, d\omega. \quad (6)$$

Using Parseval's theorem, the acoustic energy density  $E_a$  is given by

$$E_a = \int_{-\infty}^{\infty} |P_a(\omega)|^2 / (2\pi\rho c) \, d\omega. \quad (7)$$

### C. The Stationary Thermoacoustic Array

In the stationary case, the source-receiver distance  $r_0$  is a constant.

This allows Eq. (5) to be considerably simplified, giving

$$P_a(\omega) = (k C_a D_a / r_0) \exp(ik[r_0 - \alpha r_0]) \int_{-\infty}^{\infty} \omega_0(t) \exp(-ikct) \, dt. \quad (8)$$

The integral in Eq. (8) is recognized as a Fourier integral. Therefore the result may be expressed in terms of the Fourier transform of the optical power

function  $\Psi_0(\omega)$

$$P_a(\omega) = (k C_a D_a / r_0) \exp(ikr_0 - \alpha r_0) \Psi_0(\omega), \quad (9)$$

which is identical to Eq. (1). This confirms that the expression for the acoustic signal in Eq. (5) is valid for both moving and stationary cases.

#### IV. THE EFFECT OF MOVEMENT ON THE OPTICAL ENERGY REQUIREMENT

To examine the effect of movement on the optical signal requirements, let us turn Eq. (5) around and keep the acoustic signal constant. Assuming that the signal may be uniquely defined by its Fourier transform, this problem is equivalent to that of examining the factors affecting the Fourier transform of a given acoustic signal. The energy requirement analysis will start with the long range case where the MTA is moving at a constant Mach number relative to the receiver. The term "long range" is used to indicate the situation where source-receiver distance is such that the launch and arrival angles of the sound rays do not change significantly over the duration of the signal. Then, the results will be generalized to include the case of varying Mach number. Finally, the long range requirement is relaxed. In all cases, the receiver is assumed to be in the farfield of the source.

Let us consider the long range case where the MTA is traveling at a constant Mach number relative to the receiver. Referring to Fig. 1, the mean position of the MTA is centered at the origin of a Cartesian coordinate system, and the receiver is located in the x-z plane. It is assumed in the long range case that the MTA path length is small compared to the source-receiver distance; therefore changes in the source-receiver distance and the depression angle are negligibly small compared to their mean values,  $r_0$  and  $\theta_0$ . It also follows that the y component of the MTA velocity has a negligible effect on the Mach number. In this case, Eq. (5) may be approximated by

$$P_a(\omega) = (k C_a D_a / r_0) \exp(ikr_0 - \alpha r_0) \int_{-\infty}^{\infty} \omega(t) \exp(ik[v_x t \cos(\theta_0) - ct]) dt, \quad (10)$$

where  $v_x$  is the component of the MTA velocity in the x direction. The integral in Eq. (10) is recognized as a Fourier integral and it may be expressed as the Fourier transform of  $\omega(t)$ , giving

$$P_a(\omega) = (k C_a D_a / r_0) \exp(ikr_0 - \alpha r_0) W(\omega(1-M)), \quad (11)$$

where

$$M = (v_x/c) \cos(\theta).$$

#### A. The $M \neq 1$ Case

Comparing Eqs. (9) and (11) for the case where  $M \neq 1$ , the difference between the optical power signals in the stationary and moving cases can be clearly seen. In order to obtain the same acoustic signal, the latter must be a Doppler shifted version of the former,

$$W(\omega(1-M)) = W_0(\omega). \quad (12)$$

If the total optical energy expended to produce a given acoustic signal can be somehow reduced through movement of the thermocoustic array then there would be a gain in conversion efficiency. Consider the total optical energy

which is given by

$$W(\omega) = \int_{-\infty}^{\infty} w(t) dt. \quad (13)$$

The total optical energy is recognized as the Fourier transform of the optical power at  $\omega=0$ . Since a Doppler shift influences the Fourier transform at all values of  $\omega$  except at  $\omega=0$ , there should be no difference in the Fourier transforms at  $\omega=0$ , that is,

$$W(\omega) = W_0(\omega). \quad (14)$$

Substituting from Eq. (14) into (13), it is clear that motion has no effect on the total optical energy requirement,

$$\int_{-\infty}^{\infty} w(t) dt = \int_{-\infty}^{\infty} w_0(t) dt. \quad (15)$$

The result may be extended to the varying Mach number case, where the  $x$ -coordinate of the MTR is generally represented by the function  $x(t)$ . The Fourier transform of the acoustic signal is now given by

$$P_a(\omega) = (k c_a D_a / r_0) \exp(ikr_0 - \alpha r_0) \int_{-\infty}^{\infty} w(t) \exp(ik[x(t) \cos(\theta_n) - ct]) dt. \quad (16)$$

In this case, the optical power function  $w(t)$  needs to be nonuniformly Doppler shifted to maintain the same acoustic signal. If the nonuniform Doppler shift is

one that changes smoothly as a function of time, then it may be approximately broken down into a number of discrete time intervals in which the Doppler shifts are uniform,

$$P_a(\omega) \approx (k c_a D_a / r_0) \exp(ikr_0 - \alpha r_0)$$

$$-\infty \int^{\infty} \sum_{n=1}^N \omega_n(t) \exp(ik[u_{xn} t \cos(\theta_0) - ct]) dt, \quad (17)$$

where

$$\omega_n(t) = \begin{cases} \omega(t) & \text{if } t_n < t < t_{n+1} \\ 0 & \text{otherwise} \end{cases}$$

and

$$u_{xn} = (x(t_{n+1}) - x(t_n)) / (t_{n+1} - t_n).$$

The approximation becomes more exact as the number of time intervals tends to infinity. Since it has been concluded that uniform Doppler shifts do not affect the optical energy requirement, it follows that the total optical energy requirement summed over all the time intervals, where the Doppler shift in each interval is uniform, must also be unaffected.

$$\sum_{n=1}^N \omega_n(0) = \omega_0(0), \quad (18)$$

Therefore, Eq. (15) remains valid and the optical energy requirement remains unchanged.

Finally, the analysis may be broadened to include the general farfield case where changes in  $r$  and  $\theta$  cannot be considered as small. Equation (5) may be rewritten in a form similar to Eq. (16),

$$P_a(\omega) = (k C_a D_{ac} / r_0) \exp(ikr_0 - \alpha r_0) \int_{-\infty}^{\infty} \omega(t) (D_a/D_{a0}) \exp(ik[r - r_0 - ct] - \alpha(r - r_0)) dt. \quad (19)$$

In this case, the optical power function  $\omega_0(t)$  must not only be distorted to compensate for the changing Doppler shift, it must also be further distorted to compensate for the differential changes in the diffraction loss,  $(D_a/D_{a0})$ , and absorption loss,  $\exp(-\alpha(r - r_0))$ . Since the losses are range dependent and the range may change significantly over the path of the MTR, the comparison between the moving and stationary cases is not straightforward. However, since  $r_0$  and  $\theta_0$  are mean values of  $r$  and  $\theta$  over the significant part of the path, the net increase or reduction in the required optical input to maintain the same acoustic signal must be a second order quantity. Therefore, the optical energy requirement is unchanged at least to the first order of accuracy.

#### B. The M=1 Case

Let us now examine the behavior of the MTR when the Mach number  $M$  is equal to unity. From Eq. (11), it can be seen that the value of the  $\omega(\omega(1-M))$ , for all finite values of  $\omega$ , is equal to  $\omega(0)$ . That is, the optical excitation

appears to collapse into an impulse. Consequently, in the absence of any distortions, the acoustic waveform would be the derivative of an impulse.<sup>2</sup> The acoustic signal is obtained by setting  $M=1$  in Eq. (11),

$$P_a(\omega)_{M=1} = (k C_a D_a / r_0) \exp(ikr_0 - \alpha r_0) W(0). \quad (20)$$

Note that the signal is dependent only on the optical energy  $W(0)$ . Therefore, the shape of the optical power waveform has no influence on the acoustic output. The acoustic waveform is only determined by the frequency dependence of the diffraction loss  $D_a$ , which is controlled by the physical dimensions of the thermoacoustic source, and the absorption coefficient  $\alpha$ . However, this does not mean that the thermoacoustic conversion efficiency of an MTR traveling at Mach 1 will be any higher than that of a stationary TR.

In the case of a stationary TR, an identical result can be obtained by using an optical impulse. In this case, the Fourier transform of the optical power  $W_0(\omega)$  will be equal to  $W_0(0)$  for all significant values of  $\omega$ . Substituting into Eq. (9),

$$P_a(\omega)_{\text{impulse}} = (k C_a D_a / r_0) \exp(ikr_0 - \alpha r_0) W_0(0). \quad (21)$$

From Eqs. (20) and (21), it is evident that if the optical energies are equal, i.e.,  $W(0) = W_0(0)$ , then the Fourier transforms of the acoustic signals, hence the acoustic waveforms themselves, must be identical. Consequently, it is concluded that a stationary TR energized by an optical impulse would produce

exactly the same acoustic signal as an MTR, moving at  $M=1$  in the direction of the receiver, for the same optical energy. The signals will be identical in both waveform and energy density.

Substituting from Eq. (20) or (21) into Eq. (7), an expression for the acoustic signal energy density may be obtained,

$$E_a = c_0^2 (2\pi\rho c)^{-1} r_0^{-2} W(\Omega)^2 k^2 \eta_0^2 \exp(-2\alpha r_0) d\omega. \quad (22)$$

Note that the Fourier transform of the optical power input may be brought outside the integral because it is constant for all significant values of frequency. The expression also shows that if the absorption coefficient  $\alpha$  were finite and independent of frequency, and the diffraction loss  $D_0$  increases with frequency by a rate less than the second power, then the acoustic energy density  $E_a$  would be infinite. In practice, however,  $\alpha$  monotonically increases with frequency and this alone is sufficient to ensure that the acoustic energy density is always bounded. In practice, the diffraction loss  $D_0$  also increases rapidly with frequency beyond a cutoff frequency determined by the physical dimensions of the array. There are also other losses not represented, such as that due to finite amplitude effects, which would further limit the acoustic energy density at the receiver.

## U ANALYSIS OF VIABILITY AS AN ACOUSTIC PROJECTOR

### A. Upper Bound of the Energy Density

Since it has been demonstrated in the foregoing sections that thermoacoustic conversion by stationary and moving sources are equivalent, the upper bound derived below will be applicable to both cases. It is possible to obtain an upper bound for the value of the energy density,  $E_a$ , by using the fact that the term  $D_a$  in Eq. (5) and subsequent equations is a loss term and its value is always less than unity. Thus, setting  $D_a$  equal to unity in Eq. (9) and substituting into Eq. (7), the upper bound may be expressed by the following inequality,

$$E_a < (c_a/r_0)^2 (2\pi pc)^{-1} \int_{-\infty}^{\infty} k^2 \exp(-2\alpha r_0) |\mathcal{W}(\omega(1-M))|^2 d\omega. \quad (23)$$

It can be seen that the Fourier transform of the optical signal,  $\mathcal{W}(\omega(1-M))$ , at nonzero values of the acoustic signal frequency, ( $\omega \neq 0$ ), has a direct influence on the acoustic energy density but no direct connection with the optical energy input. On the other hand, the value of  $\mathcal{W}(\omega(1-M))$  at  $\omega=0$ , which represents the total optical energy, has no direct effect on the generation of the acoustic signal. Since these two Fourier transform components are mutually exclusive, it is conceivable that an acoustic signal can be generated without any net optical energy dissipation. However, in practice, this is not achievable because negative thermal power dissipation, i.e., the absorption of thermal power from the water by the laser beam, is not possible.

The value of  $W(\omega(1-M))$  at  $\omega=0$  represents a positive energy bias which allows the thermal power changes necessary for acoustic generation to take place without reversing the direction of optical power flow in the laser beam.

Under this restriction, it can be shown that the value of  $W(\omega(1-M))$  at  $\omega \neq 0$  cannot be greater than the value at  $\omega=0$ , i.e.,

$$|W(\omega(1-M))| \leq W(0) \quad \text{for} \quad \omega \neq 0. \quad (24)$$

The proof is given in Appendix B. Substituting from Eq. (24) into Eq. (23), the acoustic energy density upper bound is obtained in terms of the optical energy,  $W(0)$ ,

$$E_a < (c_a/r_0)^2 (2\pi\rho c)^{-1} W(0)^2 \int_0^\infty k^2 \exp(-2\alpha r_0) d\omega. \quad (25)$$

The upper bound given by Eq. (25) is valid in all cases, including the  $M=1$  case. For narrowband signals, the upper bound may be more exactly expressed in terms of the mean wave number,  $k_0$ , and the acoustic bandwidth,  $B_a$  (in Hz),

$$E_{a \text{ narrowband}} < ((c_a/r_0)^2 / (\rho c)) W(0)^2 k_0^2 \exp(-2\alpha r_0) 2B_a. \quad (26)$$

For a given bandwidth,  $B_a$ , and range,  $r_0$ , there is an optimum frequency at which the narrowband upper bound is at a maximum. Using the absorption curve for seawater at  $10^\circ\text{C}$ , a plot of the optimum frequency as a function of range was computed as shown in Fig. 2. The signal bandwidth was assumed to

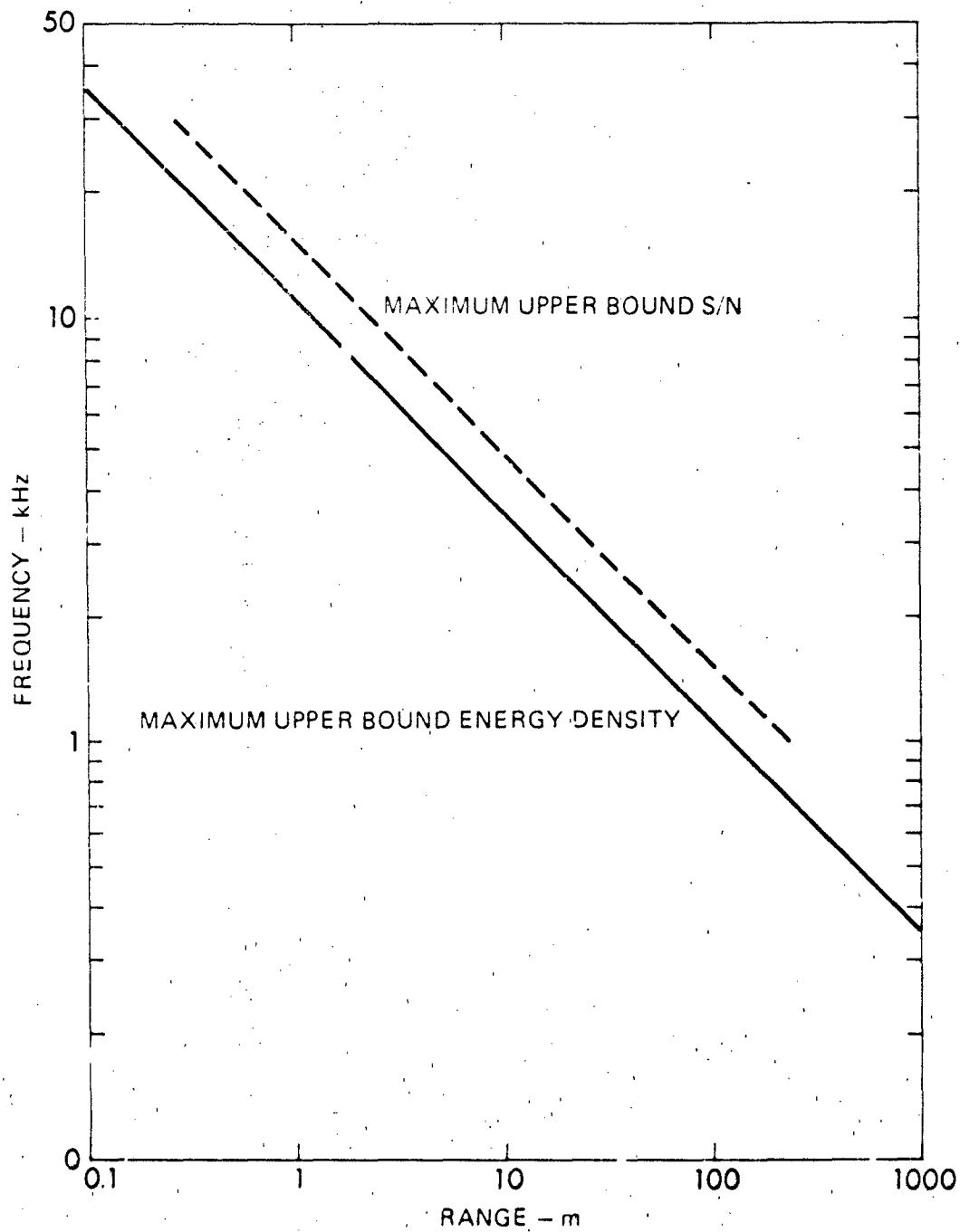


**FIGURE 2**  
**FREQUENCIES AT WHICH UPPER BOUNDS OF ENERGY DENSITY**  
**AND SIGNAL-TO-NOISE RATIO ARE MAXIMIZED**  
**THE NOISE IS ASSUMED TO BE KNUDSON NOISE,**  
**WHICH INCREASES AT 17 dB PER DECADE OF FREQUENCY**

be a constant.

### B. Waveform and the Energy Conversion Efficiency $M \neq 1$

In Eq. (23), it is evident that the acoustic signal energy density is generated by the square of the magnitude of the optical power Fourier transform,  $W(\omega(1-M))$ . Therefore, the conversion efficiency of waveforms is directly governed by the relative value of  $W(\omega(1-M))$  within the signal band to the optical energy  $W(0)$ . For a given acoustic signal, the conversion efficiency is maximized by maintaining the desired values of  $W(\omega(1-M))$  while minimizing the optical energy bias  $W(0)$  as much as possible. The most efficient optical signal is one that achieves the equality in Eq. (24) over the significant part of the signal band. In Table I, the peak values of  $W(\omega(1-M))$  within the signal band are compared for three representative waveforms; in each case  $W(0)$  is set equal to unity. The waveforms are the sine wave, the square wave, and the impulse train as shown in Fig. 3. In each case, it is assumed that the signal band is centered on the fundamental frequency  $\omega_0$ .

It is clear that, of the three waveforms, the impulse train produces the maximum acoustic signal energy for the same optical energy. It appears to be the most efficient waveform for thermoacoustic generation in general as long as unwanted harmonics do not interfere with the desired signal. Furthermore, it is well suited to laser technology where Q-switching methods for producing high energy impulses are well developed.

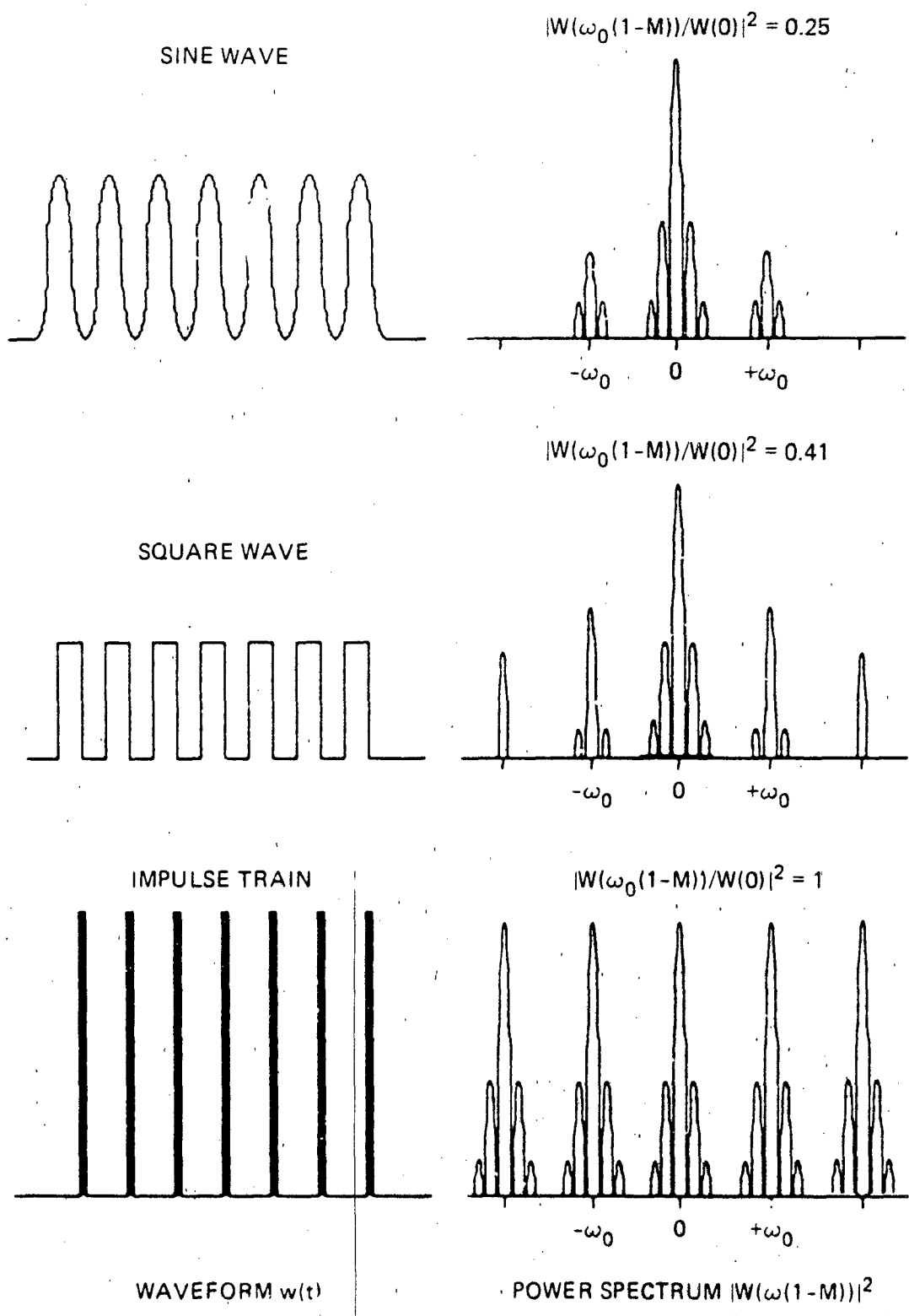


FIGURE 3  
THREE WAVEFORMS AND THEIR POWER DENSITY SPECTRA

TABLE I  
THE FUNDAMENTAL COMPONENTS OF CERTAIN PERIODIC WAVEFORMS

Waveform	$ \mathcal{W}(\omega_0(1-M)) ^2$ at $\mathcal{W}(0) = 1$
sine wave	0.25
square wave	0.41
impulse train	1.00

**C. Maximization of the Signal-to-Noise Ratio**

Consider an ideal situation where there are no boundaries, the speed of sound is constant and isotropic, the background noise is isotropic, and the receiver employs a matched filter to maximize the signal-to-noise ratio (S/N). For a one way transmission between an acoustic source and receiver, the S/N may be simply expressed by the following equation .

$$S/N = 10\log(E_B) - 10\log(F_N) + D_L \quad (27)$$

The contribution from the acoustic source in this equation is summed up in the acoustic energy density term,  $E_B$ . For a receiver of a predetermined directivity index or for an omnidirectional receiver, the S/N is maximized by maximizing the ratio  $E_B/F_N$ . For narrowband signals, there is a carrier frequency at which the upper bound S/N is a maximum. Using the expression for the upper bound signal energy density in Eq. (26), and assuming that the receiver is in a Knudson

noise limited situation where the equivalent plane wave noise spectrum increases at a rate of 17 dB per decade, the carrier frequency at which the S/N upperbound is maximized is shown as a function of range in Fig. 2.

#### D. Conversion Efficiency Upper Bound

Let us define efficiency,  $\eta$ , as the acoustic energy,  $W_a$ , produced per unit of optical energy input,  $W(0)$ . Since the sound is assumed to be radiated downwards from the surface, the acoustic energy upper bound is equal to the energy density given by inequality (25), without the absorption loss term, integrated over a hemispherical boundary below the water surface,

$$W_a < (c_a^2 / (\rho c)) W(0)^2 \int_{-\infty}^{\infty} k^2 d\omega. \quad (28)$$

The efficiency upper bound is then found by dividing the acoustic energy by the optical energy,

$$\eta < (c_a^2 / (\rho c)) W(0) \int_{-\infty}^{\infty} k^2 d\omega. \quad (29)$$

From the above inequality, it appears that, in the absence of diffraction loss and any other type of losses internal to the thermoacoustic source, the efficiency upper bound is infinite. This is clearly erroneous since it contradicts the law of conservation of energy. The flaw lies in the assumption that the medium reacts to the application of heat by expanding instantaneously. While this assumption is valid over the band of detectable acoustic frequencies, it will

break down beyond a cutoff frequency determined by the lag time of the thermal expansion process. The cutoff frequency will effectively make the limits of the integral in Eq. (29) finite and constrain the efficiency upper bound to a value less than or equal to one.

From the above analysis, it can be seen that the efficiency upper bound varies over a wide range of values, depending on acoustic signal frequency. It is seen that for high frequency sonar (e.g., 30 kHz) and reasonable optical energy levels (e.g., 100 J), the efficiency upper bound is around  $10^{-6}$ , which is marginally useful. The range penetration of a signal in this category is discussed later. At long range sonar frequencies (e.g., 3 kHz), and at reasonable levels of optical energy (e.g., 100 J), the efficiency upper bound is less than  $10^{-9}$  (and even with 1000 J of optical energy it is still less than  $10^{-8}$ ).

For narrowband signals the efficiency is significantly lower than that allowed by the upper bound, since efficiency increases with bandwidth. The expressions for total acoustic energy and efficiency are a little simpler since it is reasonable to approximate the value of the wave number by a constant over the passband. The expression for the total acoustic energy upper bound is obtained from inequality (28) by replacing the integral with a simple product,

$$W_{\text{a narrowband}} < (c_a^2 / \rho c) W(0)^2 k_0^2 4\pi B_a \quad (30)$$

The efficiency upper bound is then given by

$$\eta_{\text{narrowband}} < (c_a^2 / \rho c) W(0) k_0^2 4\pi B_a \quad (31)$$

As the  $k_0^2$  term suggests, the gains are concentrated at the high frequency end of the spectrum. In the laboratory, where operating frequencies are generally higher and propagation distances shorter than in the sea, the TA promises to be a very efficient and useful tool.<sup>7</sup> In sonar applications, however, absorption will very rapidly eliminate the high frequency components before any useful distance can be covered. The efficiency upper bounds of a TA at certain values of frequency and optical energy, assuming that the bandwidth  $B_a$  is one-half of the carrier frequency, are shown in Fig. 4.

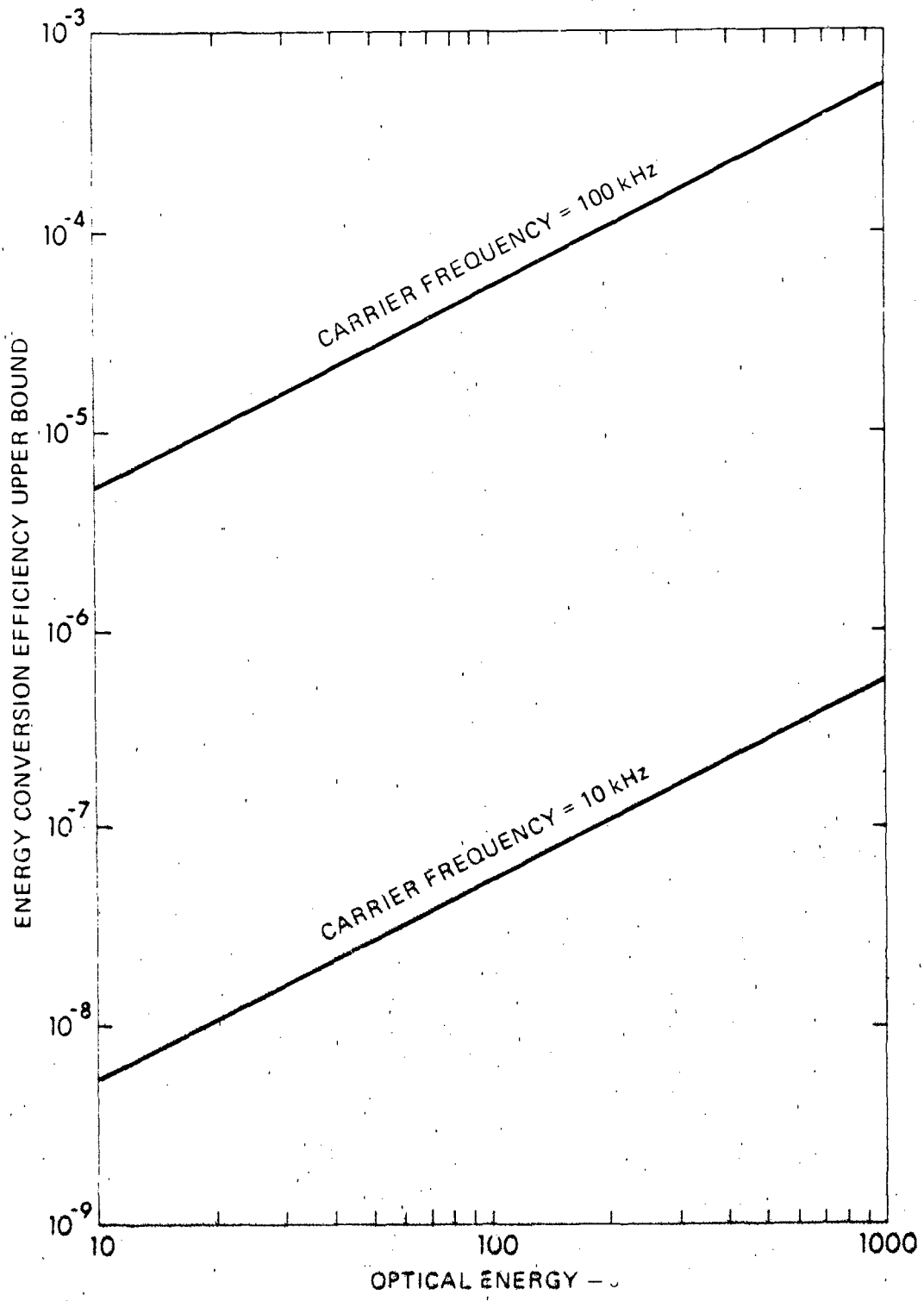


FIGURE 4  
 ENERGY CONVERSION EFFICIENCY UPPER BOUND IN SEAWATER  
 AT A TEMPERATURE OF 10°C

#### VI. NUMERICAL EXAMPLES OF MOVING THERMOACOUSTIC ARRAYS

The following numerical example will be used to set the main characteristics of the MTA into proper perspective. For this purpose, an MTA was modeled for the following set of operating conditions :

The heat source was a laser directed vertically downwards. The laser beam profile was Gaussian shaped with a  $1/e$  radius of 8 mm. The laser delivered a total of 190 J of optical energy at a wavelength of 1.06  $\mu\text{m}$ , in a train of ten pulses at a repetition rate of 2 kHz. The MTA traveled at  $M=0.9$  along the x axis giving the acoustic signal a Doppler shifted frequency of 20 kHz in the forward (+x) direction. The water was assumed to be seawater at a temperature of 10<sup>0</sup>C with an isotropic noise spectrum equivalent to that of sea state 4. The acoustic signal was received by an omnidirectional hydrophone equipped with a matched filter.

The energy density of the signal as a function of range and direction was computed. The one-way slant range penetration contour for an S/N at the receiver of 20 dB is shown on Fig. 5. The computations showed that, at a depression angle of 8<sup>0</sup> in the forward direction, the range penetration reaches a maximum value of 1400 m. The acoustic source level was computed to be 165 dB re 1  $\mu\text{Pa}$ .

By numerically integrating the energy density of the acoustic signal over a hemispherical boundary, the total energy conversion efficiency was computed

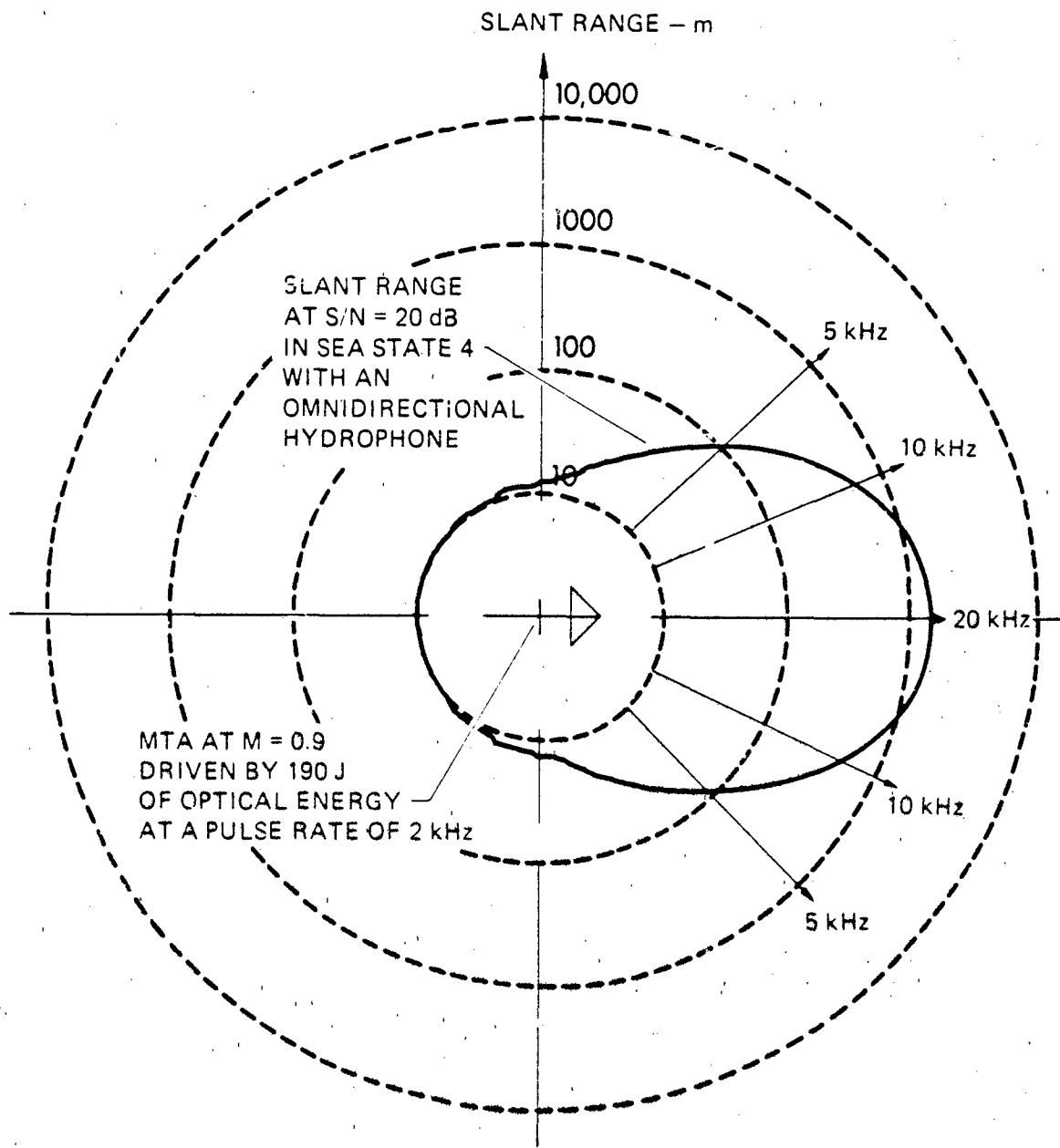
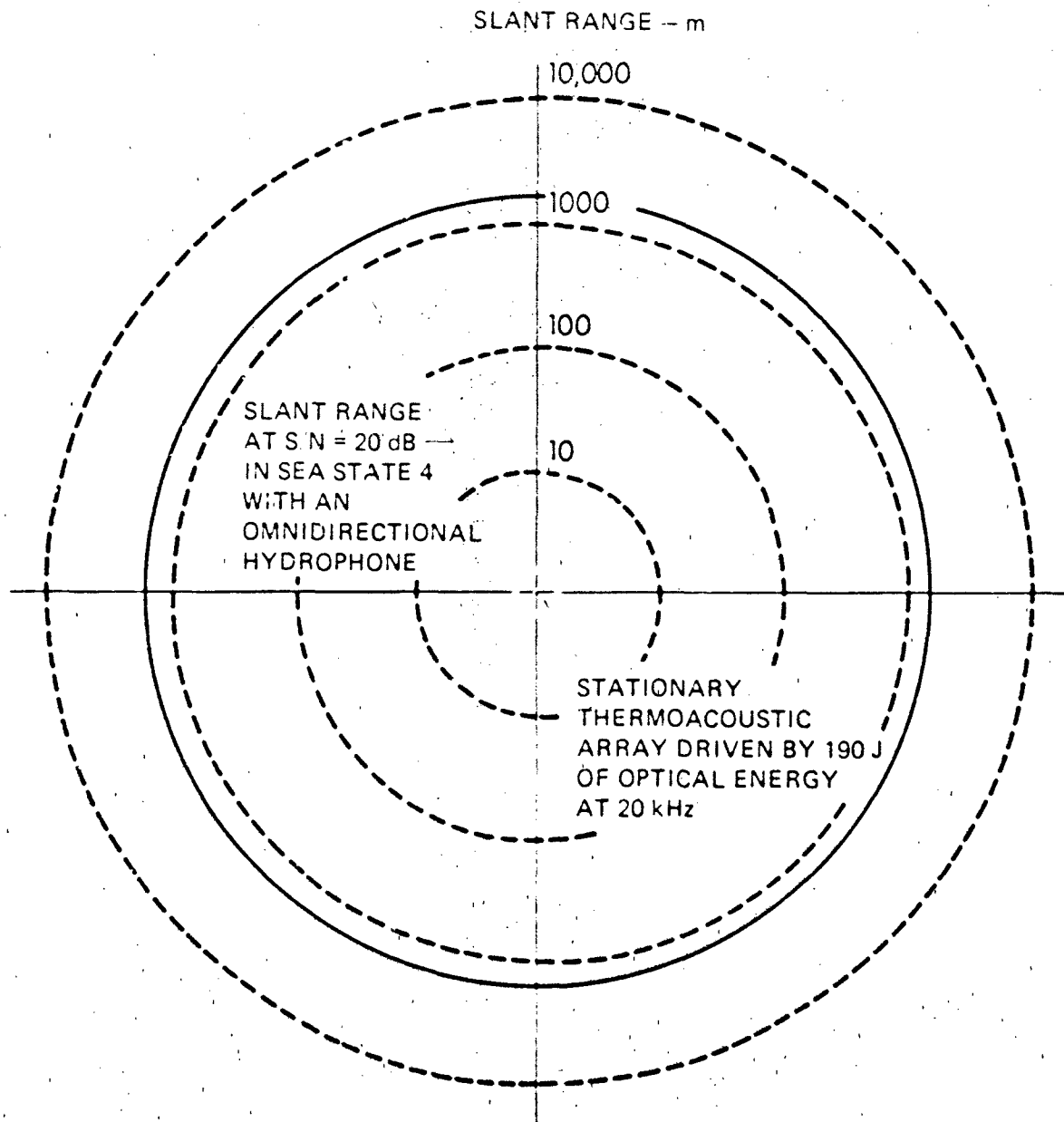


FIGURE 5  
 THE COMPUTED SLANT RANGE PENETRATION OF A MOVING THERMOACOUSTIC  
 ARRAY (MTA), TRAVELING AT M = 0.9 IN THE INDICATED DIRECTION

to be  $1 \times 10^{-8}$ . From Eq. (31), the upper bound of efficiency at a carrier frequency of 20 kHz and a bandwidth of 2 kHz is estimated to be  $1.6 \times 10^{-7}$ . Therefore, the actual efficiency is considerably less than the upper bound. The discrepancy is due to the reduction in carrier frequency as a function of angle away from the forward direction, and to diffraction loss.

The range penetration of a stationary TA pulsed at a frequency of 20 kHz, operating under the same conditions and of equal optical energy, is shown in Fig. 6. It is seen that the stationary TA has the same acoustic signal frequency of 20 kHz and achieves the same range penetration as the MTA. In the stationary case, the acoustic output is independent of azimuth. It has greater coverage but no directivity. The total energy efficiency was computed to be  $1.5 \times 10^{-7}$ . The discrepancy between the computed efficiency and the upper bound of  $1.6 \times 10^{-7}$  is due to diffraction loss. Although the stationary TA achieves better overall efficiency than the MTA, the gain is in directions other than the forward direction. The level of the 20 kHz signal in the forward direction is unaffected.

An indication of the range penetration of the acoustic signal as a function of its frequency can also be extracted from Fig. 5. The direction and range penetration of the 10 kHz and the 5 kHz signals are shown. Since the range penetration has been shown to be the same whether the thermoacoustic source is moving or stationary, the following conclusion is applicable for both cases. The results suggest that, for the given optical energy of 190 J, the range penetration below 20 kHz decreases as the frequency is reduced, in spite of the lower absorption loss at lower frequencies. This is because the



**FIGURE 6**  
**THE COMPUTED SLANT RANGE PENETRATION OF A STATIONARY**  
**THERMOACOUSTIC ARRAY GENERATING AN ACOUSTIC SIGNAL AT 20 kHz**

reduction in efficiency (plus the increase in ambient noise) outweighs the reductions in absorption loss. Further numerical analysis showed that the range penetration peaked at 20 kHz, and that beyond 20 kHz it declined with increasing frequency. Therefore, it is concluded that at an energy level of 190 J (or less) a thermoacoustic source, moving or stationary, will not provide the range penetration required for medium or long range communications.

## VII. DIRECTION FINDING CAPABILITY

In spite of its inefficiency, the MTA has a potentially useful but little explored property, and that is the property that the Doppler shift is direction dependent. This may be used as a means of direction discrimination. Since the MTA is a noncontact projector, it can move at speeds that would be quite impossible for sources that have to be in physical contact with the medium. Therefore, the range of realizable Doppler shifts can be extremely large. This should lead to a high angular resolution capability. The variation of Doppler shift with direction is given by Eq. (11) for the constant velocity case. For the general case, it is necessary to obtain a numerical solution using Eq. (5).

An example is shown in Fig. 5, where the carrier frequency of the signal from an MTA has been calculated at various azimuth angles. The MTA is traveling at  $M=0.9$  along the  $x$  axis. Along the forward direction, the signal frequency is 20 kHz due to the Doppler shift, but the frequency rapidly falls off away from the forward direction. At  $24^\circ$  from the forward direction, the frequency has already dropped to 10 kHz. With a signal bandwidth of 2 kHz, there are five resolution cells in the  $24^\circ$  sector. There is a left-right ambiguity which needs to be resolved, but that may be resolved by using an asymmetrical path or by changing the direction of movement from ping to ping.

### VIII. FINDINGS

1. The acoustic signal is directly a function of the modulation of the optical power. The total optical energy has no direct effect but it must be sufficiently large to allow the modulation components to exist. This is generally true except when the optical input is an impulse, or if the source velocity component in the direction of the receiver is equal to the sound velocity.
2. When the optical input is an impulse, or if the source velocity in the direction of the receiver is equal to the sound velocity, the acoustic signal is a function of the total optical energy and the dimensions of the source only. Any modulation of the optical power has no effect.
3. The moving thermoacoustic source is, at any speed, neither more nor less efficient than the stationary source of the same dimensions and optical energy.
4. The impulse train is the most efficient optical power waveform for the thermoacoustic generation of signals.
5. The efficiency upper bound is extremely low for practical values of optical energy and carrier frequency.
6. The direction dependent Doppler shift of the acoustic signal gives the moving thermoacoustic source a unique property which cannot be reproduced by conventional transducers and which is potentially useful for direction finding without having to use a beamformer.
7. As a laboratory tool, where propagation distances are short and operating frequencies are high, the TA can be a very useful tool particularly because of its noncontact property and wideband

capability.

8. For sonar applications, a more efficient optoacoustic conversion process is required.

### III. DISCUSSION

These findings contrast sharply with some of the claims made for the efficiency of the MTR. There are mainly two reasons.

(1) When comparing the efficiencies of transducers, it is necessary to define the desired operating conditions and then measure their efficiencies under the same conditions. To make direct comparisons of efficiencies measured under different conditions would be analogous to comparing apples and oranges. One important aspect of the operating conditions is the acoustic signal itself. For conventional transducers, valid comparisons can be made if the input signals and the other relevant operating conditions are the same, because the output signal is normally a reasonable replica of the input signal. This, however, is not the case for MTRs, which can move at speeds very much higher and hence generate far greater Doppler distortions than conventional contact transducers can ever achieve. Therefore a conscious effort must be made to generate the same acoustic signal before any meaningful efficiency comparisons can be made. In some instances,<sup>8</sup> while comparing conversion efficiencies, the acoustic signal was allowed to change with the velocity of the MTR while the optical (input) signal was kept constant and it was then concluded that the efficiency of an MTR was higher than that of a stationary TR. This conclusion is erroneous, because the conversion efficiency for generating the same acoustic signal was not compared. The correct conclusion should have been that the efficiency varied as a function of the acoustic signal used. This mistake is easy to make since, as stated above, certain assumptions that one normally takes for granted are not valid for moving

sources.

(2) In the case of the claims by Bozhkov,<sup>3,4</sup> the argument is reproduced as follows.

"The efficiency ... increases directly as the laser intensity. For a stationary source, ... laser intensity is limited by boiling of the liquid in the heating zone. In the case of the moving source the heat absorbed in the liquid is distributed in space, whereupon the ultimate value of the light intensity and, hence, the ultimate efficiency of energy conversion is greater ... than for a stationary source."

This claim is refuted as follows. First of all, it is the energy density that is limited by the boiling point and not the intensity. However, in the case of water, there is an incentive to get as close to the boiling point as possible without actually causing the liquid to boil because the coefficient of expansion,  $\beta$ , which directly governs the conversion efficiency, increases with temperature. Furthermore, should the peak laser energy density be greater than that which is consistent with maximum efficiency without boiling, it is possible to reduce and control it by widening the laser beam in a way that will not increase the diffraction loss in the desired signal direction, thereby obtaining a directional acoustic beam in the same process.

Although the MTA is no more efficient than the stationary TA, it does have one significant advantage. The Doppler shift of the signal is direction dependent. This property may be used for direction finding. Since it is easy to achieve extremely high velocities, much higher than that achievable with transducers that have to be in contact with the water, the potential angular resolution may be quite impressive.

## R. CRITICAL ISSUES

### A. Efficiency Enhancement

Clearly, the efficiency of the thermoacoustic process is too low to be useful in sonar applications except at very short ranges. A radically different process that has the advantages of remote deployment and noncontact with the water is needed. The so-called nonlinear optoacoustic process<sup>9</sup> is worth investigating. High efficiencies (up to 10%) have been claimed for it, although this may be somewhat over optimistic. It has been investigated by several researchers,<sup>9-13</sup> but the results published so far are not applicable to the sonar application.

As a first attempt, a simple blast model should be used to predict the acoustic output of the optoacoustic process. A possible candidate blast model is that of R. N. Pirri<sup>14</sup> who successfully used it to model the momentum transfer between a high power laser blast on the surface of a solid.<sup>15</sup> A more complicated model has been reported but it is essentially a one-dimensional model<sup>16</sup> developed for solid surfaces.

### B. Planned Work

The blast model needs to be developed and verified experimentally under controlled laboratory conditions. Reliable quantitative measurements of the optoacoustic sound generation process have so far not been found in the published literature. The reported works have been either qualitative<sup>10,11</sup> or

concerned with impulse generation,<sup>12,13</sup> where most of the energy is spread over a band of several megahertz, with one exception,<sup>17</sup> where the experimental conditions appeared to be imprecise. A Q-switch driver will be purchased in the fall of 1984 to enable the laser to deliver short pulses of sufficient intensity to generate blasts. Experiments will be carried out to measure the acoustic output and its spectrum. From the experimental results, a more realistic model of the optoacoustic conversion process may be obtained. Then a reliable estimator of system performance versus laser power requirements can be constructed for further evaluation.

APPENDIX A

BASIC THERMOACOUSTIC GENERATION THEORY

The acoustic pressure may be derived from the inhomogeneous wave equation

$$\Delta p_a - (\partial^2 p_a / \partial t^2) c^{-2} = -\partial q(t-r/c) / \partial t. \quad (A.1)$$

For a thermoacoustic source, the source function  $q(t)$  is given by

$$q(t) = -\nabla \cdot I(x, y, z, t) H / c_p. \quad (A.2)$$

For a stationary TA whose axis passes through the origin slanted at an angle  $\theta_1$  relative to the vertical, directed at an azimuth angle  $\phi_1$  relative to the x axis, and an intensity profile  $I_s(x, y, t)$  at the surface,

$$\nabla \cdot I(x, y, z, t) = R I_s(x_w, y_w, t) \mu \exp(-\mu z / \cos(\theta_1)), \quad (A.3)$$

where

$$x_w = x - z \cos(\phi_1) \sin(\theta_1)$$

and

$$y_w = y - z \sin(\phi_1) \sin(\theta_1).$$

It is assumed that the medium reacts to the thermal input instantaneously.

Taking the Fourier transform of Eq. (A.1),

$$\Delta P_a(\omega) + k^2 P_a(\omega) = R \mu c H / c_p \exp(-\mu z / \cos(\theta_1)) k I_s(x_w, y_w, \omega). \quad (A.4)$$

where

$$k = \omega/c,$$

$$P_a(\omega) = -\infty \int^{\infty} p_a(t) \exp(i\omega t) dt,$$

and

$$I_s(x_w, y_w, \omega) = -\infty \int^{\infty} I_s(x_w, y_w, t) \exp(i\omega t) dt.$$

Solving Eq. (A.4) for the farfield solution, the following expression is obtained for the acoustic pressure Fourier transform,

$$P_a(\omega) = A\mu cH/c_p \int_{-\infty}^{\infty} \int_{-\infty}^{\infty} \int_{-\infty}^{\infty} G(r', r_0) \exp(-\mu z/\cos(\theta_1)) k I_s(x_w, y_w, \omega) dx dy dz, \quad (A.4)$$

where

$$G(r', r_0) = \exp(-ik|r_0 - r'| - \alpha r)/(4\pi|r_0 - r'|) + \rho_{aw} \exp(-ik|r_0 - r''| - \alpha r)/(4\pi|r_0 - r''|),$$

$r''$  is the mirror image of  $r'$  in the surface, and

$\rho_{aw}$  is the acoustic reflection coefficient of the water-air surface; it is assumed to be equal to -1.

The geometry is shown in Fig. 7. Rewriting Eq. (A.4),

$$P_a(\omega) = k C_a D_a W_0(\omega) \exp(ikr_0 - \alpha r_0) / r_0, \quad (A.5)$$

where

$$\begin{aligned} W_0(\omega) &= \int_{-\infty}^{\infty} \int_{-\infty}^{\infty} w_0(t) \exp(i\omega t) dt \\ &= \int_{-\infty}^{\infty} \int_{-\infty}^{\infty} I_S(x_{WP}, y_{WP}, \omega) dx dy, \end{aligned}$$

$$C_a = Rk / (4\pi C_p),$$

and

$$\begin{aligned} D_a &= \int_{-\infty}^{\infty} \int_{-\infty}^{\infty} \int_{-\infty}^{\infty} (\mu / \cos \theta_1) \exp(-\mu z / \cos \theta_1) \\ &\quad (-G(r', r_0)) \exp(-ikr_0 + \alpha r_0) I_S(x_{WP}, y_{WP}, \omega) / W_0(\omega) dx dy dz. \end{aligned}$$

For a vertical thermoacoustic array, the value of  $\theta_1$  is zero and the expression for  $D_a$  reduces to

$$\begin{aligned} D_a &= \int_{-\infty}^{\infty} \int_{-\infty}^{\infty} \int_{-\infty}^{\infty} \mu \exp(-\mu z) \\ &\quad (-G(r', r_0)) \exp(-ikr_0 + \alpha r_0) I_S(x_{WP}, y_{WP}, \omega) / W_0(\omega) dx dy dz. \end{aligned}$$

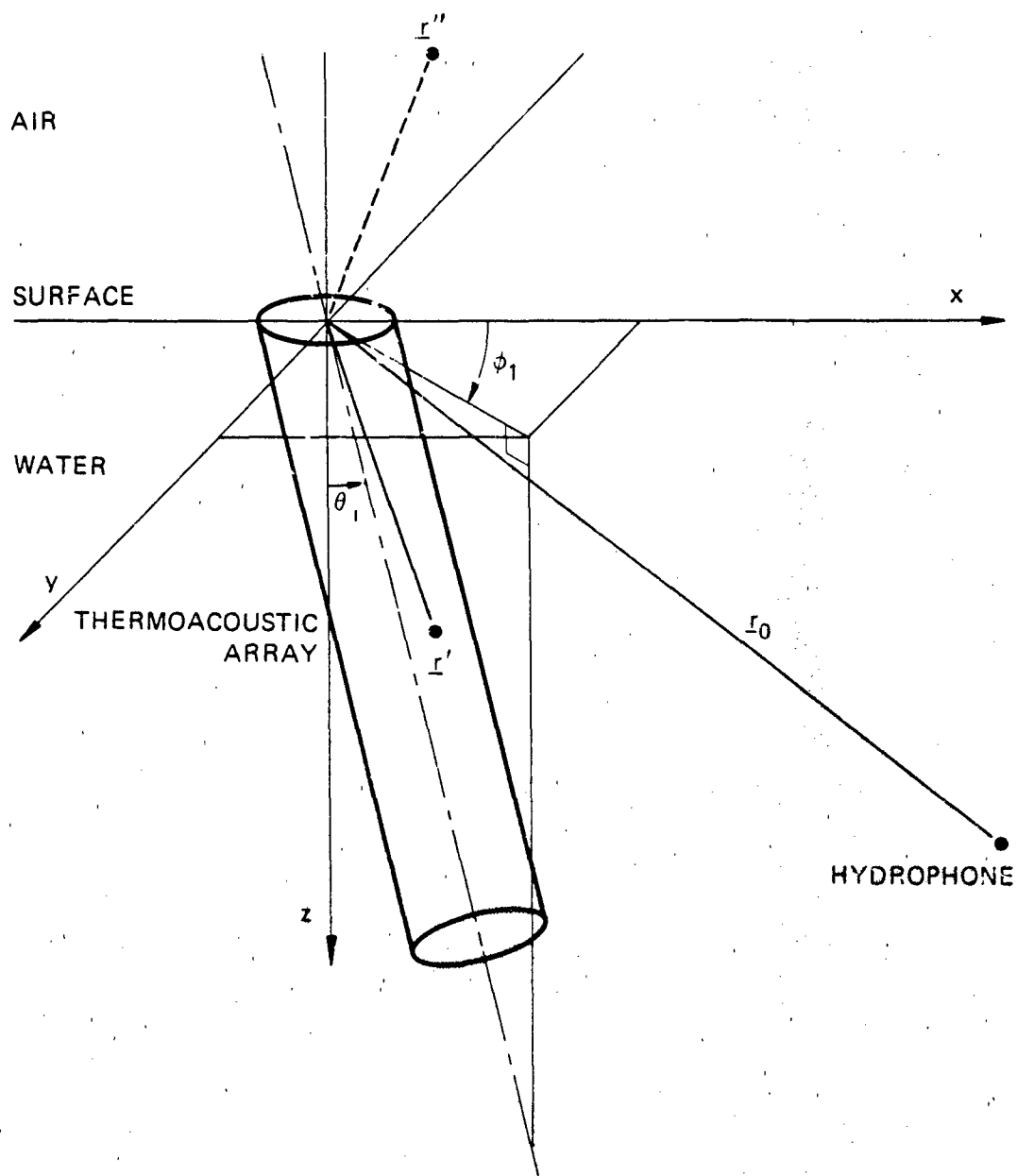


FIGURE 7  
THE GEOMETRY OF A GENERAL STATIONARY THERMOACOUSTIC ARRAY

APPENDIX B

MAXIMUM OPTICAL POWER FOURIER TRANSFORM

Given a real waveform,  $w(t)$ , and its Fourier transform,  $W(\omega)$ , and given that  $w(t)$  is greater than or equal to zero, the upper bound of the ratio  $|W(\omega)|/W(0)$  is determined as follows.

Since  $w(t) \geq 0$ , then  $w(t)$  may be expressed as the square of another function  $z(t)$ ,

$$w(t) = |z(t)|^2, \quad (B.1)$$

where  $z(t)$  is a complex waveform.

Eq. (B.1) may be rewritten as

$$w(t) = z(t) z^*(t). \quad (B.2)$$

Let  $Z(\omega)$  be the Fourier transform of  $z(t)$ . From Eq. (B.2), it follows that  $W(\omega)$  is the convolution of  $Z(\omega)$  and  $Z(-\omega)$ . Since the convolution of any function with the reverse of itself is equivalent to autocorrelation,  $W(\omega)$  is therefore the autocorrelation function of  $Z(\omega)$ . Thus

$$W(\omega) = \int_{-\infty}^{\infty} Z(\omega_1) Z^*(\omega_1 - \omega) d\omega_1. \quad (B.3)$$

For any bounded function, the peak of the autocorrelation function is real and positive and always occurs at zero displacement. Therefore,

$$W(0) \geq |W(\omega)|. \quad (B.4)$$

## REFERENCES

1. T. G. Muir, C. R. Culbertson, and J. R. Clynch, "Experiments on Thermoacoustic Arrays with Laser Excitation", *J. Acoust. Soc. Am.* 59, 735 (1976).
2. L. M. Lyamshev and L. U. Sedov, "Optical Generation of Sound in a Liquid: Thermal Mechanism (Review)", *Sov. Phys.-Acoust.* 27(1), 4-18 (1981).
3. A. I. Bozhkov, F. U. Bunkin, L. B. Esipov, A. I. Maljarovskii, and U. G. Mikhalevich, "Moving Laser Thermo-optical Sources of Ultra Sound", *Sov. Phys.-Acoust.* 26(2), 100-103 (1980).
4. A. I. Bozhkov, F. U. Bunkin, and A. A. Kolomenskii, "Doppler Thermo-optical Source of Ultrasound", *Sov. Phys.-Acoust.* 25(5), 443-445 (1979).
5. L. M. Lyamshev and L. U. Sedov, "Generation of Sound by a Moving Pulsed Optoacoustic Source", *Sov. Phys.-Acoust.* 25(6), 510-514 (1979).
6. W. H. Beyer, Ed., CRC Standard Mathematical Tables, 26th ed. (CRC Press, Florida, 1981).
7. A. C. Tam and H. Coufal, "Pulsed Opto-Acoustics : Theory and Applications", *Physique, Colloque C6, supplement au No. 10, Tome 44*, C6-9 (1983).
8. H. Hsieh and A. D. Pierce, "Some Possible Novel Configurations for Optic-Acoustic Transducer Arrays Created by Controlled Motion of Laser Beams

across Water Surfaces", presented at the 107th meeting of the Acoustical Society of America, S16(A), 6-10 May 1984.

9. L. M. Lyamshev and K. R. Naugol'nykh, "Optical Generation of Sound: Nonlinear Effects (Review)", *Sov. Phys.-Acoust.* 27(5), 357-371 (1981).

10. C. E. Bell and B. S. Maccabee, "Shock Wave Generation in Air and Water by CO<sub>2</sub> TEA Laser Radiation", *Appl. Optics* 13(3), 605-609 (1974).

11. D. C. Emmony, B. M. Geerken and A. Straaijer, "The Interaction of 10.6  $\mu$ m Laser Radiation with Liquids", *Infrared Physics* 16, 87-92 (1976).

12. E. F. Carome, C. E. Moeller, and N. A. Clark, "Intense Ruby-Laser-Induced Acoustic Impulses in Liquids", *J. Acoust. Soc. Am.* 40(6), 1462-1466 (1966).

13. P. K. Wu, "Radiation Induced Acoustic Waves in Water", *AIAA Journal* 15(12), 1809-1811 (1977).

14. R. N. Pirri, "Theory for Momentum Transfer to a Surface with a High-Power Laser", *Phys. Fluids* 16, 1435 (1973).

15. R. N. Pirri, R. Schier and D. Northam, "Momentum Transfer and Plasma Formation above a Surface with a High-Power Laser", *Appl. Phys. Lett.* 21(3), 79-81 (1972).

16. C. J. Knight, "Theoretical Modeling of Rapid Surface Vaporisation with Back

Pressure", *AIRR Journal* 17(5), 519-523 (1979).

17. G. D. Hickman and J. R. Edmonds, "Laser-Acoustic Measurement for Remotely Determining Bathymetry in Shallow Turbid Waters", *J. Acoust. Soc. Am.* 73(3), 840-843 (1983).

17 January 1985

DISTRIBUTION LIST FOR  
ARL-TR-85-3  
UNDER CONTRACT N00014-82-K-0425

Copy No.

1 Office of Naval Research  
Department of the Navy  
Arlington, VA 22217  
Attn: R. Fitzgerald

2 Director  
Naval Research Laboratory  
455 Overlook Ave., S.W.  
Washington, DC 20375  
Attn: Code 2627

3-14 Commanding Officer and Director  
Defense Technical Information Center  
Bldg. 5, Cameron Station  
Alexandria, VA 22314

15 Naval Surface Weapons Center  
White Oak Laboratory  
Silver Spring, MD 20910  
Attn: C. Beil

16 School of Mechanical Engineering  
Georgia Institute of Technology  
Atlanta, GA 30332  
Attn: A. Pierce

17 P. Rogers

18 Mechanical Engineering Department  
The University of Texas at Austin  
Austin, TX 78713  
Attn: I. Busch-Vishniac

19 D. Wilson

20 Electrical Engineering Department  
The University of Texas at Austin  
Austin, TX 78713  
Attn: M. Becker

21 Advanced Sonar Division, ARL:UT

22 Yves H. Berthelot, ARL:UT

Distribution List for ARL-TR-84-3 under Contract N00014-82-K-0425  
(cont'd)

Copy No.

23	David T. Blackstock, ARL:UT
24	Nicholas P. Chotinos, ARL:UT
25	C. Robert Culbertson, ARL:UT
26	Reuben H. Wallace, ARL:UT
27-37	Library, ARL:UT

**END**

**FILMED**

**8-85**

**DTIC**